Preprints of the 19th World Congress
The International Federation of Automatic Control
Cape Town, South Africa. August 24-29, 2014

Robust PID Control of Electrical Drive with Compliant Load ⋆

Goubej M. * **Schlegel M.** **

* *NTIS / Department of Cybernetics, University of West Bohemia, Pilsen, Czech Republic (e-mail: mgoubej@ntis.zcu.cz).*
** *NTIS / Department of Cybernetics, University of West Bohemia, Pilsen, Czech Republic (e-mail: schlegel@ntis.zcu.cz).*

Abstract: This paper deals with motion control of an electrical drive with a compliant load. Particular problem of velocity PID control is studied due to the extensive use of this control scheme in the industrial drives. The partial pole-placement method is used for the derivation of a feature-based parametrization of a set of stabilizing controllers which provide an active vibration damping functionality. Achievable quality of control is evaluated by means of proper performance indices in the form of H_∞ norm of important closed loop transfer functions. Simulation experiments demonstrate the application of the proposed method.

Keywords: motion control; active vibration control; two-mass system; PID control; mechatronics

1. INTRODUCTION

Various industrial applications of mechatronic systems such as CNC machining, rolling, assembling, welding, packaging or material handling require highly dynamic motions which have to be precisely executed by a machine (e.g. robotic manipulator, conveyor belt, machine-tool or rolling mill). Higher bandwidth of the control loops is needed in order to meet the increasing demands for precision and dynamics of the controlled motion. On the contrary, high control gains along with new types of lightweight constructions with reduced stiffness or the use of compliant components in the driven mechanisms often lead to excitation of unwanted mechanical vibrations. Such vibrations significantly reduce the overall quality of control and are recognized as the most limiting factor for the achievable bandwidth (Isermann (1997)). The motion induced oscillations complicate and prolong the process of machine commissioning and tuning of the controller gains. There is a strong demand from the industry for effective and reliable methods for the automatic or semi-automatic identification and motion control loop settings (Weißbacher et al. (2013)).

There are several approaches for modelling of vibrations in mechanical systems. Linear multi-mass models composed from set of inertial loads connected by springs and dampers are being used extensively as they can capture the oscillatory dynamics, approximate behaviour of otherwise nonlinear system around some operating point or even model an infinite dimensional system with distributed elasticity (Preumont (2011)). Two-mass system is used in this paper

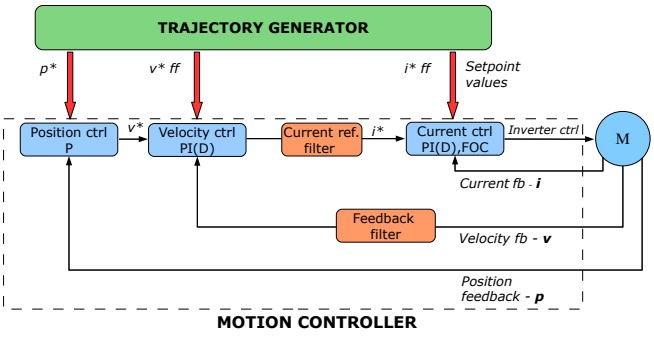

Fig. 1. **Structure of industrial motion control system**

as a general representation of rigid and first resonance modes of a compliant mechanical load.

Provided that a proper mathematical model of the controlled plant has been obtained (preferably in an automatic identification procedure), the next step is a design of a control algorithm which has to suppress the unwanted vibrations and achieve fast tracking of the reference trajectories. Passive vibration control strategies aim to reduce the gain of the control input around the resonance frequencies of the system by use of a notch filter which shapes the reference trajectory or the torque/force delivered by the actuator (Vukosavić (2007); Goubej and Schlegel (2010)). The vibrations cannot be damped in a presence of external disturbances. Active vibration control methods try to relocate the weakly damped poles of the system using a proper feedback controller. They are preferable when the resonance frequencies coincide with the range of the desired bandwidth or when the damping of vibrations caused by external disturbances is required. Various strategies have been proposed ranging from *LQG* control (Ji and Sul (1995), H_∞ control (Peter and Orlik

⋆ This paper was supported by grant TA02010247 from the Technology Agency of the Czech Republic, by the European Regional Development Fund (ERDF), project NTIS (New Technologies for Information Society, European Centre of Excellence, CZ.1.05/1.1.00/02.0090). The support is gratefully acknowledged.

(2004)), to disturbance observer (Katsura and Ohnishi (2007)), sliding-mode or model-based predictive control (Hace et al. (2007), Thomsen et al. (2011)). Such advanced methods can provide high performance for a particular system when properly tuned. However, their practical applicability is limited as the vast majority of the industrial servo controllers is equipped with the standard cascade PID structure (Fig. 1). Only motor side feedback is usually available making the problem of stabilization of compliantly coupled load difficult. Therefore, it is worthwhile to examine the performance of this standard scheme in the presence of an oscillatory load and provide some tuning rules for determination of the PID gains. Relatively low number of theoretical works deals with this problem which is very common in the industrial practice. Achievable performance of the PID controller is analyzed in (Ferretti et al. (2003); Thomsen et al. (2011). Systematic redesign based on the partial pole-placement is presented in (Zhang and Furusho (2000)) where one of the three closed-loop pole patterns is chosen based on the resonance ratio of the system. Lee et al. (2006) present two-step procedure for the robust controller design. Fictitious control for the load side is derived using a nonlinear H_∞ framework followed by a synthesis of a PID tracking controller for the motor.

This paper extends former results of the authors achieved in this field. A whole set of admissible PI(D) controllers is computed using a partial pole placement method for the nominal plant model which is acquired from an automatic identification procedure (Goubej et al. (2013); Schlegel et al. (2012)). The obtained parametrization allows fine tuning of the closed loop behaviour by adjustment of physically intuitive parameters of desired bandwidth and damping. These parameters can be adjusted manually on a real plant or by performing an optimization procedure which minimizes a suitable criterion function. Section 2 presents mathematical models of oscillatory systems. Section 3 deals with the controller synthesis followed by simulation experiments and final conclusions.

2. MATHEMATICAL MODEL

The two-mass model is a basic representation of a compliant mechanical load (Fig. 2). A motor inertia I_m is connected to a load inertia I_L by a flexible shaft. Compliance of the shaft may be modelled as a linear torsional spring described by the stiffness constant k and internal viscous friction coefficient b. The equations of motion can be formed by using Newton's laws:

$$\varepsilon_m = \dot{\omega}_m = \frac{1}{I_m}\{T_m - k(\varphi_m - \varphi_l) - b(\omega_m - \omega_l)\} \quad (1)$$
$$\varepsilon_l = \dot{\omega}_l = \frac{1}{I_l}\{k(\varphi_m - \varphi_l) + b(\omega_m - \omega_l) + T_l\}.$$

The corresponding state space model is obtained as

$$\dot{\boldsymbol{x}} = \begin{bmatrix} \dot{\omega}_m \\ \dot{\omega}_l \\ \dot{T}_s \end{bmatrix} = \begin{bmatrix} -\frac{b}{I_m} & \frac{b}{I_m} & -\frac{1}{I_m} \\ \frac{b}{I_l} & -\frac{b}{I_l} & \frac{1}{I_l} \\ k & -k & 0 \end{bmatrix} \boldsymbol{x} + \begin{bmatrix} \frac{1}{I_m} & 0 \\ 0 & \frac{1}{I_l} \\ 0 & 0 \end{bmatrix} \begin{bmatrix} T_m \\ T_l \end{bmatrix}$$
$$y = [\,1\ 0\ 0\,]\,\boldsymbol{x}, \quad (2)$$

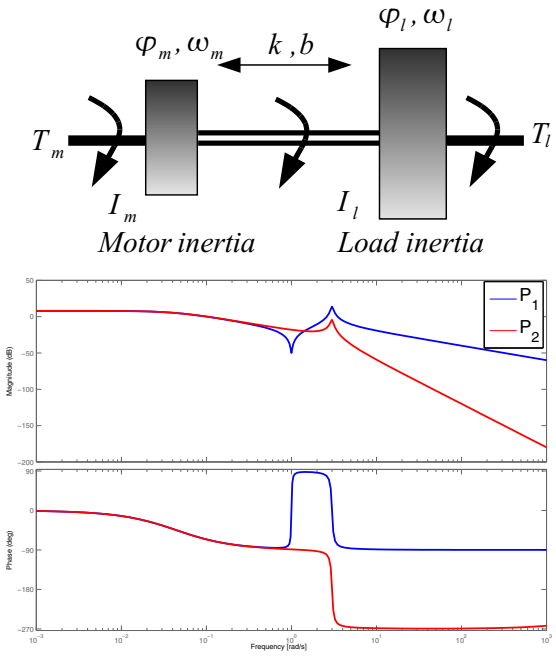

Fig. 2. **Two mass system** - rotor and load inertia coupled by a flexible shaft, typical shape of open loop Bode plots

where $\omega_{m,l}$ denote the motor and load angular velocity, T_m is the electromagnetic torque produced by the motor, T_l is the disturbance load torque and $T_s = k(\varphi_m - \varphi_l)$ is the torsional shaft torque. Only the motor side measurement is usually available in typical industrial applications.

The transfer functions from the motor torque to the motor and load speed can be obtained as

$$P_1(s) = \frac{\omega_m(s)}{T_m(s)} = \frac{I_l s^2 + bs + k}{s[I_m I_l s^2 + b(I_m + I_l)s + k(I_m + I_l)]} = \\ = \frac{K_1}{s}\frac{s^2 + 2\xi_z\omega_z s + \omega_z^2}{s^2 + 2\xi\omega_n s + \omega_n^2}, \quad (3)$$
$$P_2(s) = \frac{\omega_l(s)}{T_m(s)} = \frac{bs + k}{s[I_m I_l s^2 + b(I_m + I_l)s + k(I_m + I_l)]} = \\ = \frac{K_2}{s}\frac{s + \frac{\omega_z}{2\xi_z}}{s^2 + 2\xi\omega_n s + \omega_n^2} \approx \frac{1}{(I_m + I_l)s}\frac{\omega_n^2}{s^2 + 2\xi\omega_n s + \omega_n^2},$$

where the corresponding gains, natural frequencies and damping factors can be expressed in terms of the system parameters

$$K_1 = \frac{\omega_n^2}{(I_l + I_m)\omega_z^2},\ \omega_n = \sqrt{\frac{k(I_l + I_m)}{I_l I_m}},\ \omega_z = \sqrt{\frac{k}{I_l}}$$
$$K_2 = \frac{2\xi_z\omega_n^2}{(I_l + I_m)\omega_z},\ \xi = \sqrt{\frac{b^2(I_l + I_m)}{4kI_l I_m}},\ \xi_z = \sqrt{\frac{b^2}{4kI_l}}. \quad (4)$$

The parameter of so called *resonance ratio* is defined as

$$r = \frac{\omega_n}{\omega_z} = \frac{\xi}{\xi_z} = \sqrt{1 + R},\ R = \frac{I_l}{I_m}. \quad (5)$$

where R is the *load to drive inertia* ratio.

Higher number of resonance modes can be modelled by adding more inertial masses in the chain. The resulting transfer functions have a form

$$P_1(s) = \frac{\omega_m(s)}{T_m(s)} = \frac{K_1}{s}\frac{\prod_{i=1}^{n}(s^2 + 2\xi_{zi}\omega_{zi}s + \omega_{zi}^2)}{\prod_{i=1}^{n}(s^2 + 2\xi_i\omega_i s + \omega_i^2)}, \quad (6)$$

$$P_2(s) = \frac{\omega_l(s)}{T_m(s)} \approx \frac{K_2}{s}\frac{1}{\prod_{i=1}^{n}(s^2 + 2\xi_i\omega_i s + \omega_i^2)}, \quad (7)$$

where n is the number of masses and corresponding resonance modes.

A viscous friction can be added both to the motor and load side leading to the transfer functions:

$$P_1(s) = \frac{\omega_m(s)}{T_m(s)} = \frac{I_l s^2 + (b + b_l)s + k}{a_3 s^3 + a_2 s^2 + a_1 s + a_0}, \quad (8)$$

$$P_2(s) = \frac{\omega_l(s)}{T_m(s)} = \frac{bs + k}{a_3 s^3 + a_2 s^2 + a_1 s + a_0} \quad (9)$$

$$a_3 = I_l I_m,\ a_2 = \{I_l(b + b_m) + I_m(b + b_l)\},$$

$$a_1 = \{b_m(b_l + b) + k(I_m + I_l) + b_l b\},\ a_0 = k(b_l + b_m)\,,$$

where b_m, b_l denote motor and load friction coefficients. A typical shape of the open-loop frequency response is shown in Fig. (2). Usual values of the damping observed in industrial motion control applications with compliant loads is $\xi, \xi_z \approx 0.01..0.1$.

3. VELOCITY PID CONTROLLER SYNTHESIS

Most of the industrial motion controllers use the standard cascade PID control scheme (Fig.1). The inner current loop controls the electromagnetic torque generated by the motor. Field oriented control with linear PI control is usually employed in the case of AC drives. The controller gains can be tuned according to the modulus or symmetrical optimum criterion or using the pole-placement method. The time constant of the current loop is usually negligible compared to the dynamics of the mechanical subsystem. The velocity control loop is crucial for the purpose of vibration control and its proper tuning with respect to the compliance in the attached load is necessary. Outer position loop ensures proper positioning of the load when needed. Setpoint values are obtained from higher level of trajectory generator. The advantage of the PID cascade scheme is low number of parameters, a possibility of successive tuning of individual loops and a simple introduction of the physical limitations on maximum torque, velocity and position.

PI control

The starting point is a PI velocity controller which is implemented in most of industrial servo-drives. The closed-loop dynamics cannot be freely assigned without an additional feedback from the load velocity and shaft torque. Only two closed-loop poles out of the total four can be chosen for system (3). The location of the uncontrolled poles is determined by plant parameters and the choice of the assigned pole pair. As was shown in (Zhang and Furusho (2000)), there are fundamental limitations on the achievable closed-loop performance. Maximum bandwidth is limited by the value of antiresonance frequency and achievable damping of closed-loop poles depends on the parameter of resonance ratio r. It was observed, that systems with $r < \sqrt{2}$ cannot be damped effectively with the PI control, whereas for $r > \sqrt{5}$, the system response becomes over-damped and sluggish.

Comprehensive approach to the partial pole placement using parametric Jordan form assignment method and its application to motion control of a two-mass system was given in (Schlegel et al. (2012)). The controller synthesis problem is formulated as follows. Without loss of generality, we assume *normalized* model of the plant (3) with unitary gain and antiresonance frequency in the form of:

$$P_1(s) = \frac{\omega_m(s)}{T_m(s)} = \frac{1}{s}\frac{(s^2 + 2\xi_z s + 1)}{(s^2 + 2\xi_z r^2 s + r^2)}, \quad (10)$$

which is equivalent to the two-mass system (2) with physical parameters:

$$I_m = 1,\ I_l = k = r^2 - 1,\ b = 2\xi_z(r^2 - 1). \quad (11)$$

The normalization in gain and time simplifies the number of free parameters making the analysis and controller synthesis simpler.

We assume 2DoF PI velocity control law which can be described in the $\mathcal{L}$-domain as

$$T_m(s) = K_p\left\{w_p\omega_m^*(s) - \omega_m(s)\right\} + \frac{K_i}{s}\left\{\omega_m^*(s) - \omega_m(s)\right\}, \quad (12)$$

where ω_m^* is the setpoint value for the motor velocity and $w_p \in \langle 0, 1\rangle$ is the setpoint weighting factor of the proportional part.

Closed-loop transfer functions from the reference to motor and load speed are obtained in the form:

$$P_m^{cl}(s) = \frac{\omega_m(s)}{\omega_m^*(s)} = \frac{(w_p K_p s + K_i)\left(s^2 + 2\xi_z s + 1\right)}{s^4 + a_3 s^3 + a_2 s^2 + a_1 s + a_0}, \quad (13)$$

$$P_l^{cl}(s) = \frac{\omega_l(s)}{\omega_m^*(s)} = \frac{(w_p K_p s + K_i)\,(2\xi_z s + 1)}{s^4 + a_3 s^3 + a_2 s^2 + a_1 s + a_0}, \quad (14)$$

$$a_3 = \left(2\,\xi_z\,r^2 + K_p\right),\ a_2 = \left(2\,\xi_z\,K_p + r^2 + K_i\right),$$

$$a_1 = \left(2\,\xi_z\,K_i + K_p\right),\ a_0 = K_i.$$

Desired characteristic polynomial $a_{cl}^*(s)$ can be chosen as:

$$a_{cl}^*(s) = (s^2 + 2\xi^*\omega^* s + \omega^{*2})(s + p_3)(s + p_4), \quad (15)$$

where w_n^*, ξ^* denote desired damping and natural frequency of two assigned poles and p_3, p_4 is the second indirectly controlled pole pair.

Comparison to the closed loop polynomial in (13,14) leads to a set of polynomial equations for the unknowns K_p, K_i, p_3, p_4 which can be solved by Gröbner basis method (see Schlegel et al. (2012) for more details). Analytical solution for the PI controller gains is obtained in form:

$$K_p(\xi^*, \omega^*) = \frac{num_p(\xi^*, \omega^*)}{den_{p,i}(\xi^*, \omega^*)},\ K_i(\xi^*, \omega^*) = \frac{num_i(\xi^*, \omega^*)}{den_{p,i}(\xi^*, \omega^*)}$$

$$\begin{aligned} num_p &= 2\,\xi^*\omega^{*5} + \left(2\xi_z(1 - r^2) - 8\,\xi_z\xi^{*2}\right)\omega^{*4} + \\ &+ \left(8\,\xi^{*3} + 8\,{\xi_z}^2\xi^* r^2 - 4\,\xi^*\right)\omega^{*3} - 8\,\xi^{*2}\xi_z\,r^2\omega^{*2} \\ &+ 2\,\xi^* r^2\omega^* \\ num_i &= \omega^{*2}\{\omega^{*4} - 4\,\omega^{*3}\xi^*\xi_z + \left(4\,{\xi_z}^2 r^2 - r^2 + 4\,\xi^{*2} - 1\right)\omega^{*2} \\ &- 4\,\omega^*\xi^*\xi_z\,r^2 + r^2\} \\ den_{p,i} &= \omega^{*4} - 4\,\xi^*\xi_z\omega^{*3} - \left(2 - 4\,{\xi_z}^2 - 4\,\xi^{*2}\right)\omega^{*2} \\ &- 4\,\xi^*\xi_z\,\omega^* + 1. \end{aligned} \quad (16)$$

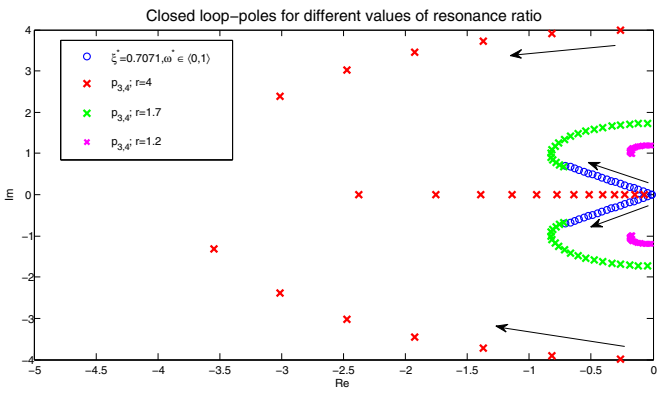

Fig. 3. **Closed loop poles for different** r

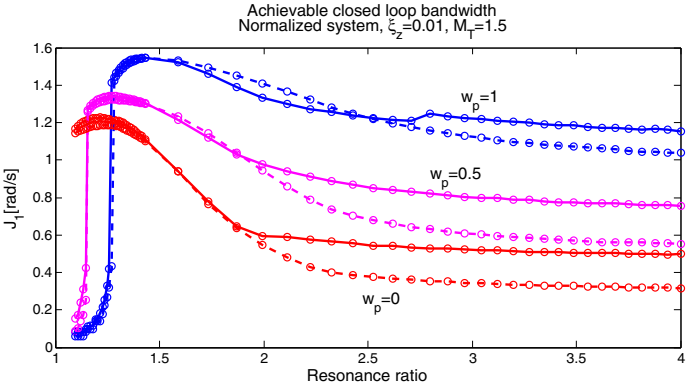

Fig. 4. **Maximum achievable bandwidth -** $J_1[rad/s]$

The controller gains are rational functions of the assigned poles location and system parameters. Stability of the closed loop with the controller (16) has to be examined, because the second pole-pair p_3, p_4 can potentially enter the right half-plane for a particular choice of ξ^*, ω^*. Hurwitz matrix can be constructed for the characteristic polynomial (13):

$$H = \begin{bmatrix} 2\xi_z r^2 + K_p & 2\xi_z K_i + K_p & 0 & 0 \\ 1 & 2\xi_z K_p + K_i + r^2 & K_i & 0 \\ 0 & 2\xi_z r^2 + K_p & 2\xi_z K_i + K_p & 0 \\ 0 & 0 & 0 & K_i \end{bmatrix}. \tag{17}$$

All the coefficients are positive for $K_p, K_i > 0$ fulfilling the necessary condition of stability. The leading principal minors of H are:

$$\begin{aligned} |H_2| =& 4\,{\xi_z}^2 K_p\, r^2 + 2\,\xi_z\,{K_p}^2 + 2\,K_i\,\xi_z\,\left(r^2-1\right) \\ & K_i\,K_p + 2\,r^4\xi_z + K_p\,\left(r^2-1\right), \\ |H_3| =& 8\,{\xi_z}^3 K_i\,K_p\,r^2 + \left(4\,K_i\,{K_p}^2 + 4\,r^2{K_p}^2\right){\xi_z}^2 \\ & + 2\,K_p\,\left(r^4 - 2\,K_i + {K_p}^2 + {K_i}^2\right)\xi_z + \\ & \left(4\,{\xi_z}^2{K_i}^2 + {K_p}^2\right)\left(r^2-1\right). \end{aligned} \tag{18}$$

Since $r > 1$, they are positive for all $K_p, K_i > 0$. Therefore, positiveness of controller gains gives sufficient condition of stability. This condition also appears from natural demand for stable and minimum-phase controller. The common denominator $den_{p,i}(\omega^*)$ of rational functions in (16) has four roots:

$$\begin{aligned} \omega^*_{1,2} &= \xi^*\,\xi_z + \sqrt{u} \pm \sqrt{2\,{\xi^*}^2{\xi_z}^2 + 2\,\xi^*\,\xi_z\,\sqrt{u} - {\xi_z}^2 - {\xi^*}^2} \\ \omega^*_{3,4} &= \xi^*\,\xi_z - \sqrt{u} \pm \sqrt{2\,{\xi^*}^2{\xi_z}^2 - 2\,\xi^*\,\xi_z\,\sqrt{u} - {\xi_z}^2 - {\xi^*}^2} \\ u &= (\xi^{*2}-1)(\xi_z^2-1) \end{aligned} \tag{19}$$

Since $u < 0$ for $\xi^* > 1$ and $\xi_z \in (0,1)$, complex roots are obtained and den_p, i is positive $\forall\omega^*$. This also holds for the case $\xi^* \in (0,1\rangle, \xi_z \in (0,1), \xi^* \neq \xi_z$ (follows from inspection of last term under the square-root), which is valid for practical cases of lightly damped systems where $\xi_z << \xi^*$). Special case $\xi^* = \xi_z \in (0,1\rangle$ leads to real roots in $\omega^* = 1$. Therefore, $den_{p,i}$ is positive and the range of applicable controller gains can be determined by inspection of numerators num_p, num_i. There are important properties of parametrization (16):

$$\begin{aligned} & K_p(\xi^*, \omega^* = 0) = 0,\ K_i(\xi^*, \omega^* = 0) = 0, \\ & \frac{\partial K_p}{\partial \omega^*} = 2\xi^* r^2, \frac{\partial K_i}{\partial \omega^*} = 0, \frac{\partial^2 K_i}{\partial {\omega^*}^2} = 2r \mid\ \omega^* = 0 \end{aligned} \tag{20}$$

Zero gains are obtained for $\omega^* = 0$ and the loop is smoothly closing when ω^* is gradually increased. There is always a nonempty range of applicable $\omega^* \in \langle 0, \omega^*_{max}\rangle$ which results in positive controller gains. This range can be found for a chosen ξ^* by computing a first real root of polynomials $num_p(\omega^*), num_i(\omega^*)$ in the admissible interval of $\omega^* \in \langle 0,1\rangle$ (follows from fundamental limitation on achievable bandwidth for the normalized plant). This can be done with use of Sturm's theorem and proper numerical method for isolation of the roots. The maximum allowable radius $\omega^*_{max}(\xi^*) \in \langle 0,1\rangle$ is the lower bound from these two limits and defines a permissible range of assignable $\omega^*(\xi^*) \in \langle 0, \omega^*_{max}\rangle$ which parameterize all stabilizing PI controllers which are stable and minimum-phase ($K_p, K_i > 0$). Computation of ω^*_{max} can be performed automatically in a drive commissioning software. However, formulas (16) can be also used for a simple manual tuning. For a chosen ξ^*, the closed loop bandwidth can be adjusted by the single parameter ω^* until a satisfactory closed loop behaviour is achieved while only positive values of K_p, K_i are accepted.

From the obtained set of stabilizing controllers given by the range $\omega^*(\xi^*) \in \langle 0, \omega^*_{max}\rangle$, one particular controller can be selected according to proper performance criterions. The first important performance index can be defined as the closed-loop bandwidth (in the standard -3dB sense) with respect to the *load motion* (14):

$$\begin{aligned} J_1 = \omega_0^{max};\ & |P_l^{cl}(i\omega)| > -3dB\ \forall\omega \in \langle 0, \omega_0^{max}\rangle \\ \cap \|P_l^{cl}(s)\|_\infty = \sup_{\forall\omega} & |P_l^{cl}(i\omega)| < M_T^{max} \end{aligned} \tag{21}$$

The limitation of maximum peak value M_T^{max} is introduced to disqualify closed loops with oscillatory behaviour or excessive overshoot due to weakly damped poles or system zeros. The achievable bandwidth is strongly affected by the resonance ratio of the system due to the differing behaviour of the unassigned pole pair (see Fig.(3), controlled poles are varied in range $\omega^* \in \langle 0,1\rangle$ for the fixed value $\xi^* = \sqrt{2}/2$, location of second pole pair is plotted for $r = 1.2, 1.7, 4$). The maximum bandwidth as a function of resonance ratio is shown in Fig.(4). Three cases of setpoint weighting factor w_p in (12) are plotted: $w_p = 1$ (blue line - 1DoF PI controller), $w_p = 0.5$ (magenta - 2DoF controller), $w_p = 0$ (red - output proportional feedback). Solid lines correspond to the setting $\xi^* = \sqrt{2}/2$, dashed lines stand for $\xi^* = 1$. It can be seen, that the achievable

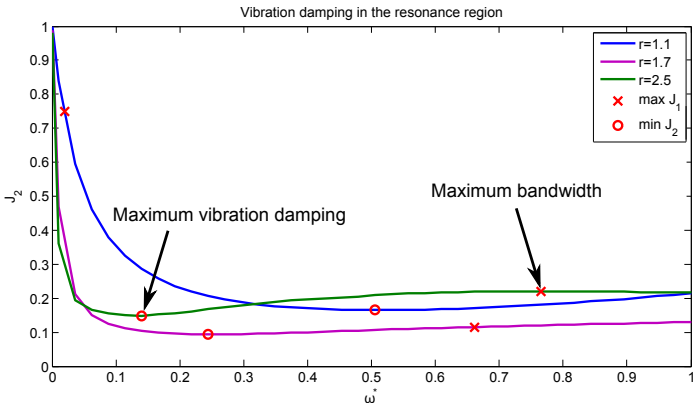

Fig. 5. **Active vibration damping - J_2**

bandwidth drops considerably for $r < \sqrt{2}$ in the case of 1DoF controller. The uncontrollable pole pair p_3, p_4 cannot be damped enough resulting in oscillatory behaviour of the closed loop. This effect is even emphasized by the real zero $z_1 = K_i/K_p$ which is introduced by the compensator in $P_l^{cl}(s)$ in the vicinity of system resonance. The range of controllable systems with low r can be extended by reduction of setpoint weighting factor w_p. The achievable bandwidth drops exponentially for large $r > 2$ due to real poles p_3, p_4 approaching the right half-plane which limit the range of applicable gains (see Fig.(3) for $r = 4$). The compensator zero for higher values of w_p is beneficial in this case as it provides a phase lead and extends the achievable bandwidth. Lower values of ξ^* leads to shorter settling times for a large r.

The second performance index is introduced for the evaluation of the active vibration damping property of the controller:

$$J_2 = \frac{\|S_l^{cl}(s)W(s)\|_\infty}{\|S_l^{ol}(s)W(s)\|_\infty} = \frac{\sup\limits_{\forall\omega}|S_l^{cl}(i\omega)W(i\omega)|}{\sup\limits_{\forall\omega}|S_l^{ol}(i\omega)W(i\omega)|}, W(s) = \frac{s}{s+r},$$

$$S_l^{cl}(s) = \frac{\omega_l(s)}{T_l(s)} = \frac{s}{r^2-1}\frac{s^2 + (2\xi_z(r^2-1) + Kp)s + (r^2 - 1 + Ki)}{a_{cl}(s)},$$

$$S_l^{ol}(s) = S_l^{cl}(s) \mid K_p, K_i = 0, \qquad (22)$$

where $a_{cl}(s)$ is closed loop characteristic polynomial from (14). The high-pass weighting filter $W(s)$ is added to emphasize the region of system resonance frequency. The normalization with respect to the open-loop is introduced to obtain a reasonable scaling of the index. The values of J_2 as a function of controller gains $\omega^* \in \langle 0, 1\rangle, \xi^* = 1$ are plotted in Fig.(5) for different values of r. Typical shape with exponential decay is caused by increasing damping of the second pole pair. Optimal performance of the controller is achieved in the range $\omega^* \in \langle min(J_2), max(J_1)\rangle$. This interval may be empty for a poorly controllable system for which the poles cannot be damped sufficiently (blue line in Fig.5).

Robust performance

Occurrence of higher resonance modes, sensor or actuator lag, sampling effects or measurement noise are typical examples of unmodeled high-frequency dynamics which limits the achievable bandwidth. The modelling errors can be expressed as a multiplicative uncertainty which perturbs the nominal plant $P_n(s)$:

$$P(s) = P_n(s)(1 + \delta(s)). \qquad (23)$$

Condition of robust stability can be derived with use of Small gain theorem as

$$\|T(s)\delta(s)\|_\infty < 1. \qquad (24)$$

where $T(s)$ is complementary sensitivity function. By looking at (13,14) and (21), it is clearly seen that the robustness in stability with respect to high-frequency perturbations is inversely proportional to the closed-loop bandwidth and criterion J_1. The same conclusion holds for the injection of a measurement noise. For a known estimate of upper bound of $|\delta(i\omega)|$, which can be obtained from an automatic identification experiment, robust controller can be designed by computing a range of applicable gains $\omega^* \in \langle 0, \omega_\delta^{max}\rangle$ for which the condition (24) holds.

PID control

Good closed-loop performance in both reference tracking and vibration control can be achieved by PI controller for well behaved systems with $r \in \langle\sqrt{2}, \sqrt{5}\rangle$. Deterioration of quality of control is observed outside of this region. Effective damping of all closed loop poles is impossible for lower r, whereas a sluggish response and low bandwidth is obtained for higher r. The performance can be improved by introduction of the derivative action of the PID controller. The derivative part can be used for adjustment of the resonance ratio. The 2DoF PID control is given as

$$T_m(s) = K_p\left\{w_p\omega_m^*(s) - \omega_m(s)\right\} + \frac{K_i}{s}\left\{\omega_m^*(s) - \omega_m(s)\right\}$$
$$+ \frac{K_d s}{\tau s + 1}\left\{w_d\omega_m^*(s) - \omega_m(s)\right\},\ w_p, w_d \in \langle 0, 1\rangle, \qquad (25)$$

where w_d is setpoint weighting factor for the derivative part and τ is low-pass filter time constant. Provided that the derivative part works effectively in the range of system resonance frequency ($1/\tau >> r$), the closed-loop dynamics may be approximated as

$$P_l^{cl}(s) = \frac{\omega_l(s)}{\omega_m^*(s)} \approx \frac{\left(w_d\frac{K_d}{K_d+1}s^2 + w_p\bar{K}_p s + \bar{K}_i\right)(2\xi_z s + 1)}{s^4 + a_3s^3 + a_2s^2 + a_1s + a_0}, \qquad (26)$$

$$a_3 = \left(2\,\xi_z\,\bar{r}^2 + \bar{K}_p\right),\ a_2 = \left(2\,\xi_z\,\bar{K}_p + \bar{r}^2 + \bar{K}_i\right), \bar{K}_p = \frac{K_p}{K_d+1},$$

$$a_1 = \left(2\,\xi_z\,\bar{K}_i + \bar{K}_p\right),\ a_0 = \bar{K}_i,\ \bar{r}^2 - 1 = \frac{r^2-1}{K_d+1}, \bar{K}_i = \frac{K_i}{K_d+1}.$$

Comparison of (26),(5) and (14) shows, that the derivative part adjusts the *virtual load to drive inertia ratio* and the corresponding resonance ratio $\bar{r}$ which can be moved to the optimal range $\bar{r} \approx \sqrt{3}..\sqrt{4}$ to achieve highest bandwidth and effective damping of closed loop poles. Positive K_d which decreases the resonance ratio should be used for slow systems with large r whereas negative values are suitable for poorly controllable systems with low r. The second case for $K_d < 0$ should be used with caution as the positive derivative feedback can destabilize the loop in case of unmodeled dynamics. Moreover, unstable zeros can be introduced in (26) in case of 1DoF controller leading to undesirable behaviour during setpoint tracking. The range of applicable derivative gain is also limited by the level of the measurement noise.

The algorithm of controller synthesis can be summarized as follows:

(1) For the normalized plant (10), compute the set of stable, minimum-phase stabilizing controllers (16)

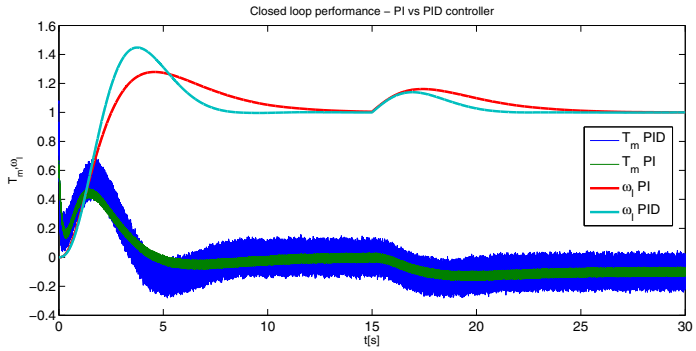

Fig. 6. **Closed loop performance** - PI and PID control

(2) Adjust the derivative part of the controller (when available) in the case of poorly controllable system to improve the resonance ratio
(3) Compute the range of optimal gains $\langle \omega^*_{J1}, \omega^*_{J2} \rangle$ according to the criterions J_1, J_2
(4) Compute the upper bound on ω^* with respect to the model uncertainty $\delta(s)$(when available)
(5) Select a particular controller from the resulting interval $\langle \omega^*_{min}, \omega^*_{max} \rangle$ as a suitable trade-off between performance and robustness.
(6) Compute the controller for the original plant by denormalization in gain and time

All these steps can be performed automatically in a drive commissioning software. The obtained parametrization can be used for the smooth fine tuning on a real plant. As an alternative to steps 2) and 3), a standard H_∞ framework formulation (e.g. the mixed sensitivity problem) can be used in the search for an optimal controller from the set obtained in step 1). The complexity of the optimization problem is vastly reduced. The algorithm can be generalized for the system with friction (8).

4. SIMULATION RESULTS

The application of the proposed method is demonstrated on a numerical example. Slow system with normalized parameters $r = 3, \xi_z = 0.005$ is to be controlled with the PI(D) compensator. Maximum damping of the dominant closed-loop poles is chosen as $\xi^* = 1$. The set of admissible PI controllers (16) with respect to J_1 (21) is obtained for $\omega^* \in \langle 0, 0.65 \rangle$. Maximum bandwidth $J_1 = 1.12 \frac{rad}{s}$ is achieved for $\omega^* = 0.65$ which leads to PI gains $K_p = 6.41, K_i = 1.37$. Closed-loop setpoint and disturbance response is shown in Fig. (6). Derivative feedback $K_d = 2, \tau = 0.125$ shifts the resonance ratio to $\bar{r} = 1.9$ and higher PI gains $\omega^* = 1, K_p = 9.89, K_i = 2.94$ may be applied. The use of PID controller leads to improvement in the closed-loop bandwidth which is increased to $J_1 = 1.44 \frac{rad}{s}$ at the cost of higher amplification of the measurement noise. The overshoot in the setpoint response could be reduced by adjustment of weighting factors w_p, w_d in the case of 2DoF controller.

5. CONCLUSION

The proposed algorithm provides a systematic approach for the synthesis of PI(D) velocity controller for an electrical drive with a compliant load. The obtained feature-based parameterization defines a set of admissible controllers, from which an optimal one can be selected according to a proper criterion function and condition of robust stability. Smooth fine tuning of the controller gains is possible using physically intuitive parameters of desired bandwidth and damping. The main intended field of application is the automatic commissioning of electrical drives in industrial applications.

REFERENCES

Ferretti, G., Magnani, G., and Rocco, P. (2003). Load behavior concerned PID control for two-mass servo systems. In *IEEE/ASME International Conference on Advanced Intelligent Mechatronics*, volume 2, 821–826 vol.2.

Goubej, M., Krejci, A., and Schlegel, M. (2013). Robust frequency identification of oscillatory electromechanical systems. In *2013 International Conference on Process Control*, 79–84.

Goubej, M. and Schlegel, M. (2010). Feature-based parametrization of input shaping filters with time delays. *IFAC Workshop on time delay systems, Prague.*

Hace, A., Jezernik, K., and Sabanovic, A. (2007). SMC with disturbance observer for a linear belt drive. *IEEE Transactions on Industrial Electronics*, 54(6), 3402–3412.

Isermann, R. (1997). Mechatronic systems - a challenge for control engineering. *Proceedings of the American Control Conference, Albuquerque, New Mexico.*

Ji, J. and Sul, S. (1995). Kalman filter and LQ based speed controller for torsional vibration suppression in a 2-mass motor drive system. *IEEE Transactions on Industrial Electronics*, 42, 564–571.

Katsura, S. and Ohnishi, K. (2007). Force servoing by flexible manipulator based on resonance ratio control. *IEEE Transactions on Industrial Electronics*, 54(1), 539–547.

Lee, S.H., Hur, J.S., Cho, H.C., and Park, J.H. (2006). A PID-type robust controller design for industrial robots with flexible joints. In *SICE-ICASE International Joint Conference*, 5905–5910.

Peter, K. and Orlik, B. (2004). H_∞ position control with robust friction compensation for a two-mass system. In *IEEE IAS Annual Meeting.*

Preumont, A. (2011). *Vibration Control of Active Structures.* Springer.

Schlegel, M., Goubej, M., and Königsmarková, J. (2012). Active vibration control of two-mass flexible system using parametric Jordan form assignment. In *2nd IFAC Conference on Advances in PID Control.*

Thomsen, S., Hoffmann, N., and Fuchs, F. (2011). PI control, PI-based state space control, and model-based predictive control for drive systems with elastically coupled loads; a comparative study. *IEEE Transactions on Industrial Electronics*, 58(8), 3647–3657.

Vukosavić, S.L. (2007). *Digital Control of Electrical Drives.* Springer.

Weißbacher, J., Grünbacher, E., and Horn, M. (2013). Automatic tuning of a servo drive speed controller for industrial applications. In *Proceedings of IEEE Conference on Mechatronics, Vicenza, Italy.*

Zhang, G. and Furusho, J. (2000). Speed control of two-inertia system by PI/PID control. *IEEE Transactions on Industrial Electronics*, 47(3), 603–609.